APPLIED SCIENCES AND ENGINEERING

Programmable transparent organic luminescent tags

Max Gmelch, Heidi Thomas, Felix Fries, Sebastian Reineke*

A milestone in the field of organic luminescent labeling is reached, as fast and multiple (>40 cycles) printing of information onto any substrate in any size for very low costs is shown, resulting in rewritable high-resolution (>700 dpi) and high-contrast images. By making use of a simple device structure containing nothing but highly available materials, an ultrathin, flexible, and fully transparent layer stack was realized. Using light alone, any luminescent image can be printed into and erased from this layer contactless and without the need of any ink. Compared to existing approaches, the demonstrated concept represents a promising method for production of luminescent on-demand tags with the potential to supersede conventional labeling techniques in many ways.

INTRODUCTION

Despite being unfamiliar to most people, phosphorescence is part of our daily lives. This type of luminescent emission shows lifetimes from microseconds (*1*) to several hours (*2*) due to a quantum mechanically small transition probability (*3*). Besides its widespread usage in glow-in-the-dark products (*4*) such as emergency sign illuminants in public buildings (*5*), it also found its way to information storage purposes like stamp detection and verification on letters (*6*). For these purposes, inorganic phosphorescent dyes such as europium-doped $SrAl_2O_4$ (*5*) are used. However, this system is powdery, requires rare earth elements, and is expensive to fabricate. Easier processing is given by organic emitters, which can simply be spin-coated (*7*), drop-casted, or evaporated (*8*) onto a variety of substrates. Developed with massive global efforts for organic light-emitting diodes (OLEDs) (*9*), they are able to show either fluorescence, phosphorescence, or both, the latter referred to as biluminescence (*10*). Yet, achieving visible organic phosphorescence under ambient conditions is not straightforward due to vibrational losses and oxygen quenching of the excited triplet states (*11*). Earlier studies have presented various methods for avoiding these nonradiative decay channels (*12*) by using, for example, aggregation (*13*, *14*) or special host molecules (*15*), some of which provide low oxygen permeability (*16*). By coating a printed document with a permanently phosphorescent layer, a very simple luminescent watermark is realized (*16*).

By combining phosphorescent and fluorescent powders, invisible luminescent content can be realized (*13*, *14*). Here, an ultraviolet (UV)– or heat-induced conformational change of the emitting molecules leads to temporary activation of phosphorescence, enabling external modification of emission features (*17*–*19*). However, powdery material is difficult to process in large-scale applications and only yields nontransparent grains, whereas neat films show high transparency and uniformity. A conformational change, however, can also lead to reversible phosphorescence in thin films (*20*). Nevertheless, a storage of complex information is not possible because of the all-or-nothing switching style causing a homogenously afterglowing layer. Single-time writing in amorphous films was realized very recently using deep UV radiation at 254 nm to cross-link polymers and therefore reducing vibrational quenching (*21*). However, the film is not transparent, the achieved image contrast is low, the printing time exceeds 1 hour, and it is not possible to print a second image after the first one disappeared.

Dresden Integrated Center for Applied Physics and Photonic Materials (IAPP) and Institute for Applied Physics, Technische Universität Dresden, 01187 Dresden, Germany.
*Corresponding author. Email: sebastian.reineke@tu-dresden.de

For labeling applications, however, multiple cycles of writing and erasing of different patterns is inevitable. A promising approach to such applications is to locally remove molecular oxygen using UV irradiation, which has been shown so far only in a liquid sample (*22*). In this case, the emitters are excited to the triplet state from where they get quenched by interaction with the triplet ground state of molecular oxygen (*23*). The resulting excited singlet oxygen interacts with surrounding solvent molecules and vanishes in the local environment of the emitter, which gives rise to phosphorescence. In this concept, choosing the right solvent is crucial, which limits its application to fluid- and gel-like substrates. Furthermore, erasing only works through liquefying, and a sample thickness of several millimeters is necessary to achieve reasonable luminescence. Progress has been made by synthesis of a polymer-based phosphorescent film (*24*). However, the opaque appearance and the deactivation of phosphorescence through water vapor injection show the narrow limits of this strategy. In addition, all mentioned strategies rely on the careful synthesis of the emitting molecules or the complex design of their conformation.

RESULTS AND DISCUSSION

Here, we present a confluence of all the features of the previously shown concepts with unmatched performance in multiple regards. We use an ultrathin emitting layer with a thickness of 900 nm, containing poly(methyl methacrylate) (PMMA; also known as acrylic glass) as host and 2 weight % (wt %) *N*,*N*′-di(1-naphthyl)-*N*,*N*′-diphenyl-(1,1′-biphenyl)-4,4′-diamine (NPB) as guest molecule. The latter is well known as a hole transport material in OLED technology (*25*–*27*) and therefore highly available. The system exhibits long-lasting room-temperature phosphorescence in the absence of oxygen, caused by moderate spin orbit coupling and the dense packing of the host polymers. The latter rigidifies the emitter and therefore leads to the reduction of nonradiative decay channels (*28*, *29*). Through spin coating, spray coating, or drop casting, it was applied from solution to multiple substrates, including transparent and flexible ones. Analogously, a 600-nm-thick oxygen-barrier layer was deposited on top of the sample to avoid exposure of the emitting layer to surrounding oxygen (Fig. 1D). Sample fabrication under ambient conditions results in the emitting layer still containing molecular oxygen.

After excitation with UV light of 365-nm wavelength, the NPB molecules reach their excited singlet state S_1 from where they either decay back to the ground state, visible as fluorescence, or populate

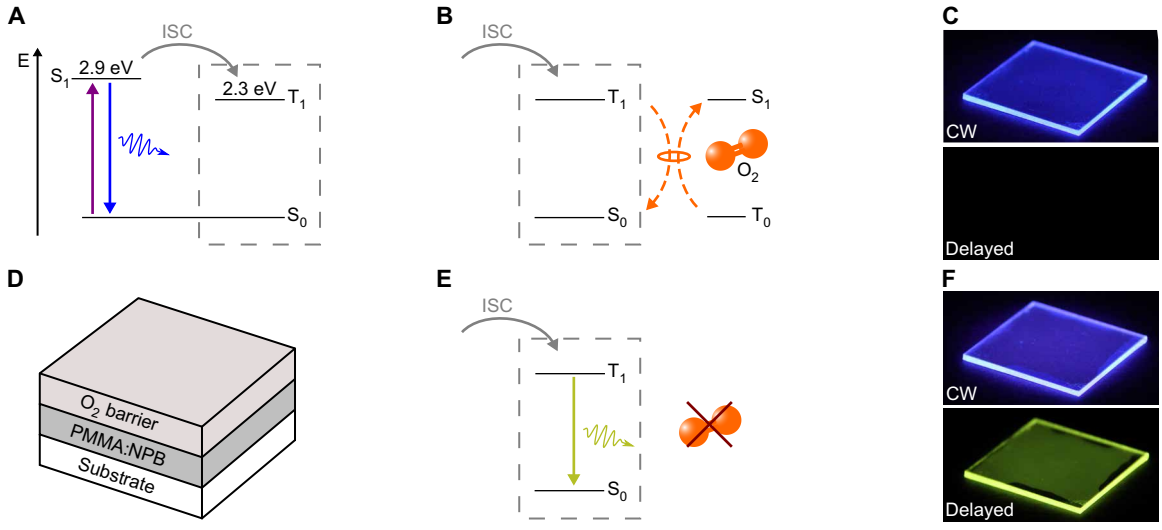

Fig. 1. Energetic scheme, device structure, and emission with and without oxygen quenching. (**A**) Electron excitation by UV light to the excited singlet state S_1 of NPB with following fluorescence or ISC to the excited triplet state T_1. (**B**) NPB T_1 state depopulation in the presence of oxygen via triplet-triplet interaction with molecular oxygen and therefore excited singlet oxygen generation. (**C**) Blue fluorescent emission in continuous wave (CW) excitation, no delayed phosphorescence in the presence of oxygen. (Photo credit: F.F., Dresden Integrated Center for Applied Physics and Photonic Materials). (**D**) Device structure. The emitting- and barrier-layer thicknesses are 900 and 600 nm, respectively. (**E**) NPB T_1 state depopulation without surrounding oxygen via visible phosphorescence with a lifetime of $\tau = 406$ ms. (**F**) Blue fluorescent emission in continuous wave excitation and delayed response in the absence of oxygen. Greenish-yellow phosphorescence is visible.

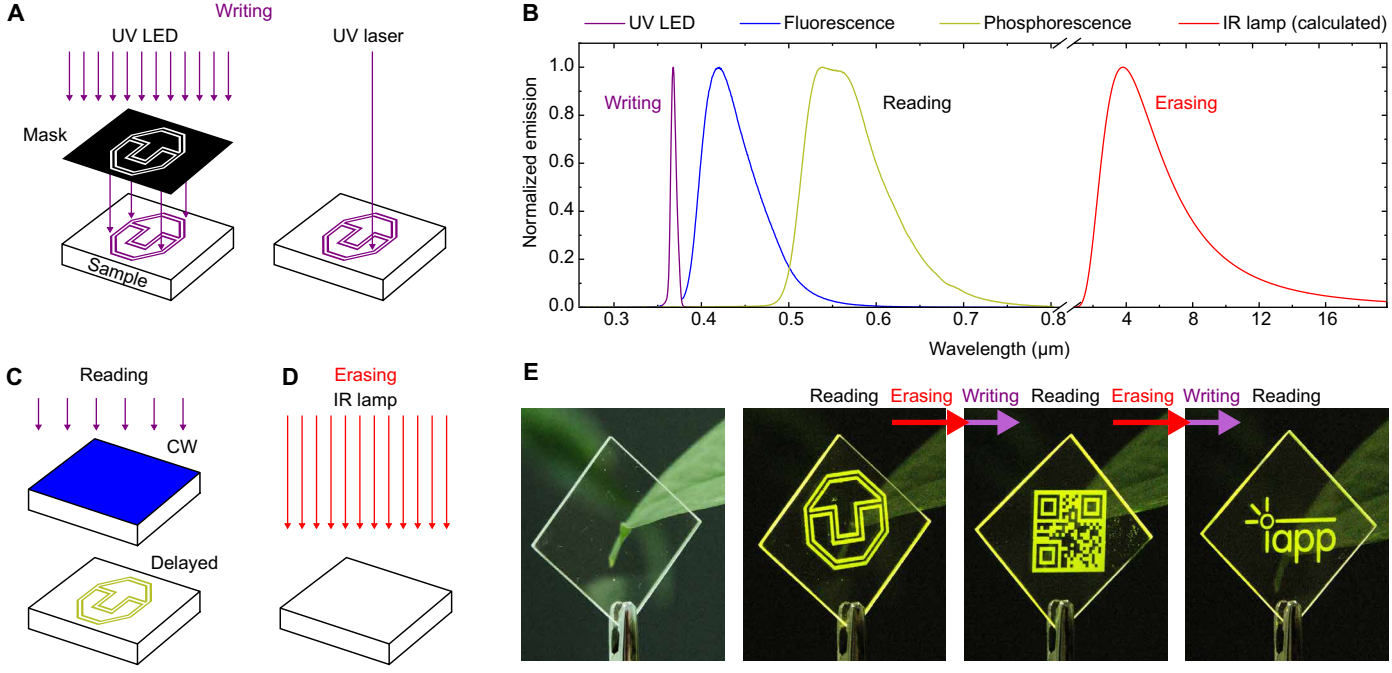

Fig. 2. Overview of writing, reading and erasing procedure. (**A**) Writing: Masked UV illumination used for the images in (E) and proposed straight laser ray writing. (**B**) Different spectral domains used for different cycle steps. Data writing is realized with a 365-nm LED, the biluminophore emits at 420 nm (fluorescence) and 530 to 570 nm (phosphorescence). IR light peaking at 4 μm is uSsed for erasing. Note that the IR spectrum is calculated from black-body radiation at 490°C. (**C**) Reading: High luminescent contrast is achieved by phosphorescence on mask-illuminated areas in delayed emission. (**D**) Erasing: By heating the sample through IR illumination, the programming is erased within around 1 min. (**E**) Different phosphorescent images written successively onto the same transparent substrate. The time span between the afterglow images is about 5 min.

the excited triplet state T_1 (Fig. 1A) through intersystem crossing (ISC) (*30*). The observed energy levels of singlet (2.9 eV) and triplet (2.3 eV) states fit well to literature values (*31*). In the presence of molecular oxygen, which has a triplet ground state T_0, the NPB T_1 state gets depopulated nonradiatively by triplet-triplet interaction of both molecules, resulting in a ground state NPB and an excited oxygen singlet state S_1 (Fig. 1, B and C) (*28*). The generated singlet oxygen gets consumed by oxidizing the PMMA (*32*). This consumption

process is observed in independent control measurements in both neat film and solution samples (fig. S1). In consequence, the density of molecular oxygen decreases locally at the illuminated spots, and as a result, phosphorescence appears (Fig. 1E). This emission is visible by eye right after switching off the UV illumination (Fig. 1F) due to the long lifetime of $\tau = 406$ ms (fig. S2). To the best of our knowledge, we realize the activation of luminescence for the first time by removing oxygen molecules from inside a neat film. This progress is crucial on the way to large-scale applications and easy handling of the materials.

The described UV-light–dependent oxygen consumption can be used as a writing tool to realize greatly improved processability and image quality compared to earlier reports (*16*–*22*, *24*). By mask illumination of the samples (Fig. 2A), any pattern can be applied as phosphorescent information storage. With the help of a focused LED spot, direct writing without the need of a mask is possible. To obtain fast and precise writing, a UV laser spot could also be used. While entirely transparent in the visible, an inscribed sample shows a highly sharp image (>700 dpi; fig. S3) in delayed emission after excitation (Fig. 2C). Furthermore, the phosphorescent image can be erased fast and easily when applying infrared (IR) light of a wavelength of ~4 μm for approximately 1 min (Fig. 2D). This radiation is well absorbed by PMMA (*33*), causing a heating up to about 90° to 100°C. This value is low enough to ensure the thermal stability of all used materials (*34*–*36*). As a result of the temperature rise, the oxygen-barrier permeability increases (*37*), and the emitting layer undergoes an oxygen refilling. During the whole erasing process, the solidity of the layers is well conserved. Subsequently, further write and erase cycles are possible (Fig. 2E). Through photo bleaching (degradation of the emitter molecules) and oxygen consumption (increased nonradiative losses due to matrix change), the intensity of phosphorescence decreases in each cycle (see fig. S4 for further details). However, after a cycle repetition of 40 times, the emission still reaches 40% of its initial value (fig. S4), which is sufficient to be easily detected by the eye or camera. In total, a fully optical accessible—writing, reading, and erasing—information storage (Fig. 2, B and E) is realized.

By initial illumination, the oxygen concentration in the emitting layer immediately starts to decrease and, at some point, is sufficiently low to enable unquenched phosphorescence (Fig. 3A). This activation process shows a power-law time dependence of the excitation light intensity with an exponent of −1 (Fig. 3B), meaning that double intensity reduces the required illumination time by a factor of 2. High excitation density of 7 mW cm^{-2} gives rise to phosphorescent emission already after 8 s. On the other hand, at low intensity of 0.1 mW cm^{-2}, the oxygen is not removed for almost 15 min. This allows both fast writing using high intensity and multiple readout repetitions without losing the imprinted structure by applying low intensity. The required intensity and time are far below the previously mentioned techniques (*17*, *21*, *22*) and therefore way more feasible for industrial application.

Because of the imperfection of the oxygen barrier, after some time, oxygen reappears in the activated areas even at room temperature. The time it takes for the phosphorescence to disappear depends on the layer thickness of the oxygen barrier. A spin-coated layer with a thickness of 600 nm preserves the phosphorescence for up to 5 hours, while a thick drop-casted film of 35 to 40 μm extends this to more than 1 day (Fig. 3C). The readout intensity was set to 0.1 mW cm^{-2} for both measurements to avoid substantial influence on the results by unintentional phosphorescence activation. The usage

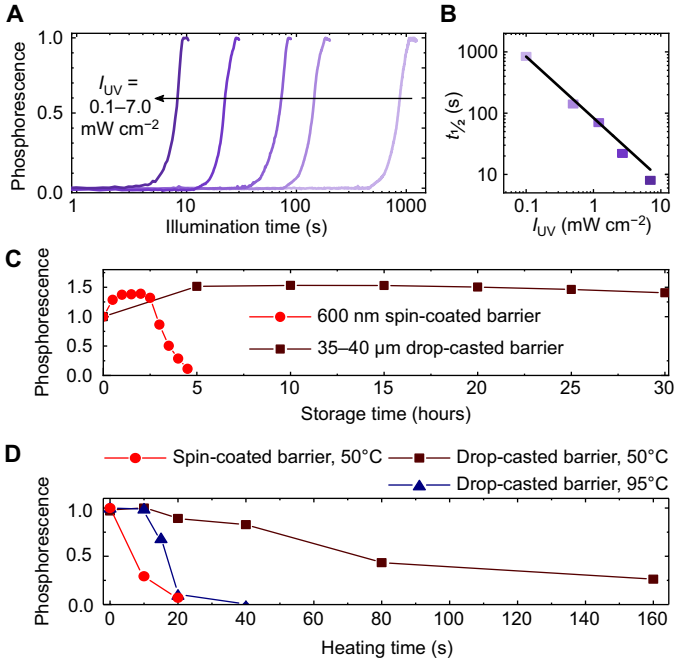

Fig. 3. Dynamics of emerging and disappearing phosphorescence. (**A**) Normalized phosphorescent intensity of freshly prepared samples as a function of illumination time for different UV intensities ranging from 0.1 to 7.0 mW cm^{-2}. (**B**) Illumination intensity dependences of required time to reach 50% of total phosphorescent emission. The black line is a power-law fit using an exponent of −1. (**C**) Normalized phosphorescence as a function of storage time for two different film thicknesses, 600 nm (light red circles) and 35 to 40 μm (dark red squares), stored and measured under ambient conditions. The emission increase at the beginning is reproducible and under further investigation. (**D**) Normalized phosphorescence as a function of heating time. Heated at 50°C, a spin-coated barrier layer leads to the loss of phosphorescence after 10 to 20 s. At this temperature, a thick drop-casted barrier layer retains phosphorescence for more than 160 s. Heated at 95°C, the same sample shows the full loss of phosphorescence after 20 to 40 s.

of an improved barrier material or further increased thickness could enhance the retention time to even higher values. For quick erasing, the oxygen refilling process is accelerated through heating the sample via IR or a simple hotplate. The time needed to delete the phosphorescence is dependent on the barrier-layer thickness and temperature (Fig. 3D). The samples were put onto a hotplate and cooled down to room temperature before measuring. While heating at 50°C for 20 s is sufficient for spin-coated layers, a drop-casted barrier still shows phosphorescence after 160 s of heating at that temperature. For heating at 95°C, this time is reduced to 20 to 40 s.

Flexible samples using self-sticking adhesive foil as substrate and a sandwich-like encapsulation, realized by a barrier layer below and on top of the emission layer, show the same writing, reading, and erasing possibilities as rigid glass platelets (Fig. 4A). Such flexible systems enable highly flexible labeling applications (Fig. 4B). A further variety of substrate materials was tested (fig. S6), including customary photographs (Fig. 4C) as large-area application. Being fully invisible when not activated, the emissive coating serves as a programmable on-demand caption. The transmission of this layer was determined with the help of a glass substrate coated similarly to the photograph by drop casting and is above 90% for the entire visible range (Fig. 4D). Thus, these coatings are more transparent than a thin glass window with a thickness of 1 mm.

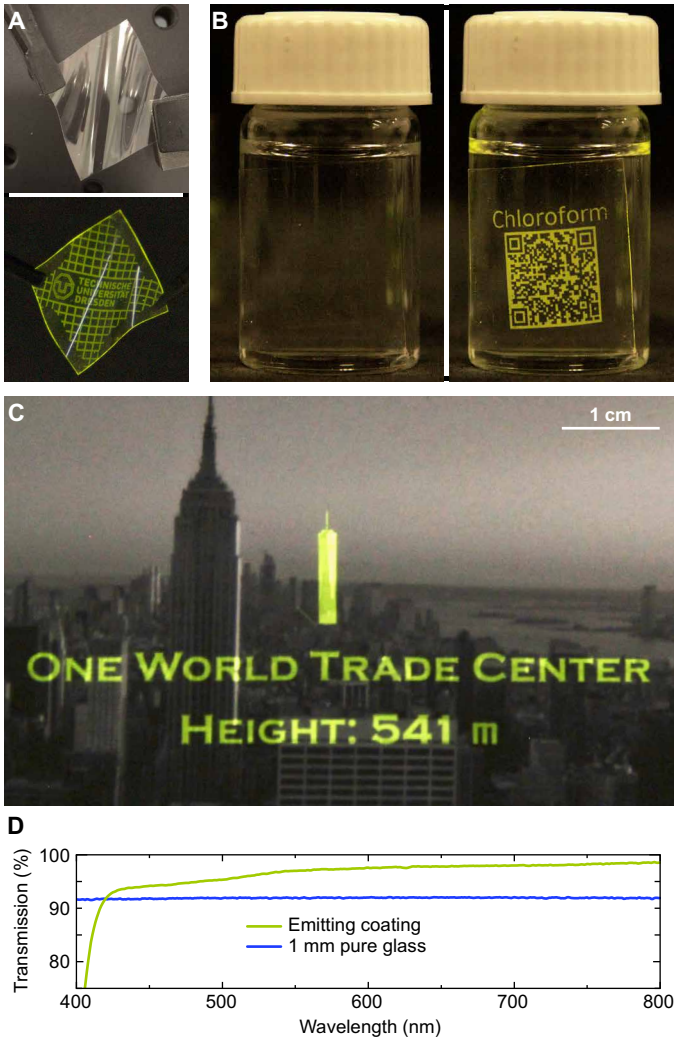

Fig. 4. Coatings on different substrates. (**A**) Flexible luminescent tag realized by spin-coating the emitting layer in between two barrier films in ambient light and showing written phosphorescence. (**B**) Flexible adhesive tag applied to a cylindrical glass bottle and containing information about the content, readable by eye and any quick response (QR) detector, and fully invisible when not read out. (**C**) Conventional monochrome photograph coated by drop-casting the emitting layer in between two barrier layers showing a programmable luminescent caption. (**D**) Transmission of an emitting layer similar to the one on top of the photo in (C) compared to 1-mm pure glass.

CONCLUSION

In conclusion, we have demonstrated the possibility of repeatable noncontact labeling and reading with resolution beyond common printer quality. Because of the small amount of highly available material required, the expense for a film of 1 m^2 is below $1.50. The presented label concept can be fabricated using highly scalable processes that are available today. The demonstrated readout resolution is sufficient for an information depth of 7 kB cm^{-2}, which is adequate to five pages of plain text. These luminescent tags therefore not only offer a previously unknown kind of information storage that goes beyond permanent data encoding but also allow for low-cost implementation and scaling. Their invisibility and implementation onto highly flexible carriers allow labeling to expand to new fields of use, starting in improved industrial logistics tracking, where tagging of single components, whole products, and transport containers takes place a million times every single day.

MATERIALS AND METHODS

Materials

NPB was purchased from Lumtec Technology Corp., and PMMA (average molecular weight 550,000) was purchased from Alfa Aesar. The oxygen-barrier material was obtained from Kuraray Europe GmbH and contains modified ethylene-vinyl alcohol copolymers as used in food packaging.

Film fabrication

Both NPB and PMMA were dissolved in anisole to reach a solution containing 2 wt % NPB and 98 wt % PMMA. The barrier material was dissolved in pure water at 95° to 130°C. For spin coating, a speed of 2000 rpm and volumes of 150 and 500 µl were used to form uniform films of emission and barrier layer, respectively. The layers were coated on top of each other. For drop casting, 150 and 500 µl were put onto the substrate for emission and barrier layer and dried overnight. The cleaned borosilicate and quartz glass substrates of a size of 25 mm by 25 mm were used as rigid substrates, while common adhesion foils were used as flexible ones. To spin-coat onto the latter, they were temporarily adhered onto glass carriers.

Optical measurements

To investigate the time-dependent phosphorescence, spectral measurements were performed using a CAS 140CTS from Instrument Systems. To trigger the detection and the 365-nm LED M365 L2 (Thorlabs), a TGP3122 pulse generator (AIM-TTI Instruments) was used. Long-term measurements were triggered by a home-built LabView software. For the time-dependent plots, each phosphorescent spectrum was integrated over wavelength. All measurements were performed in darkness. To determine the phosphorescent lifetime, a silicon photodetector PDA100A by Thorlabs was used.

IR heating

To erase the phosphorescence, an IR lamp IOT-90 purchased from Elstein-Werk M. Steinmetz GmbH and Co. KG was used. Sample temperature while heating was measured with an IR thermometer Voltcraft IR 260-8S.

Hotplate heating

To heat the samples to a defined temperature, a hotplate VWR VMS-C7 was used.

Mask fabrication

Masks were printed with a common laserjet printer onto overhead transparencies.

Resolution determination

The maximum possible resolution was determined by sample illumination through a negative USAF test target R1DS1N (Thorlabs). The photo was taken through a home-built microscope after removing the test target.

Layer thickness determination

The layer thicknesses were obtained using a Veeco Dektak 150 Profilometer.

Transmission determination

The layer, solution, and glass transmissions were measured using a Shimadzu MPC-3100. The layer transmission was measured using an empty glass substrate as reference.

Photographs

All photographs were taken with a conventional digital single-lens reflex camera EOS60D from Canon. Note that some images are slightly contrast corrected to ensure sufficient image quality when printed.

SUPPLEMENTARY MATERIALS

Supplementary material for this article is available at http://advances.sciencemag.org/cgi/content/full/5/2/eaau7310/DC1

Fig. S1. Oxygen consumption effects in solutions and films containing PMMA and NPB.
Fig. S2. Phosphorescence decay of PMMA:NPB (2 wt %) covered by an oxygen barrier.
Fig. S3. USAF 1951 test target and achieved maximum resolution.
Fig. S4. Writing and erasing cycles and resulting degradation processes.
Fig. S5. Different coating methods on different substrate materials.
Movie S1. Image writing using UV light.
Movie S2. Image reading using UV light.
Movie S3. Writing, reading, and erasing different patterns.
Movie S4. Image writing using UV light (original video).

REFERENCES AND NOTES

1. S. Lamansky, P. Djurovich, D. Murphy, F. Abdel-Razzaq, R. Kwong, I. Tsyba, M. Bortz, B. Mui, R. Bau, M. E. Thompson, Synthesis and characterization of phosphorescent cyclometalated iridium complexes. *Inorg. Chem.* **40**, 1704–1711 (2001).
2. F. Clabau, X. Rocquefelte, S. Jobic, P. Deniard, M.-H. Whangbo, A. Garcia, T. Le Mercier, Mechanism of phosphorescence appropriate for the long-lasting phosphors Eu^{2+}-doped $SrAl_2O_4$ with codopants Dy^{3+} and B^{3+}. *Chem. Mater.* **17**, 3904–3912 (2005).
3. R. S. Becker, *Theory and Interpretation of Fluorescence and Phosphorescence* (Wiley Interscience, 1969).
4. P. B. O'Hara, W. St. Peter, C. Engelson, Turning on the light: Lessons from luminescence. *J. Chem. Educ.* **82**, 49 (2005).
5. T. Matsuzawa, Y. Aoki, N. Takeuchi, Y. Murayama, A new long phosphorescent phosphor with high brightness, $SrAl_2O_4$: Eu^{2+}, Dy^{3+}. *J. Electrochem. Soc.* **143**, 2670–2673 (1996).
6. J. B. Sharkey, Chemistry of postage stamps: Dyes, phosphors, adhesives. *J. Chem. Educ.* **64**, 195 (1987).
7. L. E. Scriven, Physics and applications of DIP coating and spin coating. *MRS Online Proc. Libr.* **121**, 717–730 (1988).
8. S. R. Forrest, The path to ubiquitous and low-cost organic electronic appliances on plastic. *Nature* **428**, 911–918 (2004).
9. B. Geffroy, P. le Roy, C. Prat, Organic light-emitting diode (OLED) technology: Materials, devices and display technologies. *Polym. Int.* **55**, 572–582 (2006).
10. C. Salas Redondo, P. Kleine, K. Roszeitis, T. Achenbach, M. Kroll, M. Thomschke, S. Reineke, Interplay of fluorescence and phosphorescence in organic bilumineSCent emitters. *J. Phys. Chem. C* **121**, 14946–14953 (2017).
11. A. Garner, F. Wilkinson, Quenching of triplet states by molecular oxygen and the role of charge-transfer interactions. *Chem. Phys. Lett.* **45**, 432–435 (1977).
12. M. A. Filatov, S. Baluschev, K. Landfester, Protection of densely populated excited triplet state ensembles against deactivation by molecular oxygen. *Chem. Soc. Rev.* **45**, 4668–4689 (2016).
13. Z. An, C. Zheng, Y. Tao, R. Chen, H. Shi, T. Chen, Z. Wang, H. Li, R. Deng, X. Liu, W. Huang, Stabilizing triplet excited states for ultralong organic phosphorescence. *Nat. Mater.* **14**, 685–690 (2015).
14. S. Cai, H. Shi, J. Li, L. Gu, Y. Ni, Z. Cheng, S. Wang, W.-w. Xiong, L. Li, Z. An, W. Huang, Visible-light-excited ultralong organic phosphorescence by manipulating intermolecular interactions. *Adv. Mater.* **29**, 1701244 (2017).
15. S. Hirata, K. Totani, J. Zhang, T. Yamashita, H. Kaji, S. R. Marder, T. Watanabe, C. Adachi, Efficient persistent room temperature phosphorescence in organic amorphous materials under ambient conditions. *Adv. Funct. Mater.* **23**, 3386–3397 (2013).
16. Y. Deng, D. Zhao, X. Chen, F. Wang, H. Song, D. Shen, Long lifetime pure organic phosphorescence based on water soluble carbon dots. *Chem. Commun.* **49**, 5751–5753 (2013).
17. L. Gu, H. Shi, M. Gu, K. Ling, H. Ma, S. Cai, L. Song, C. Ma, H. Li, G. Xing, X. Hang, J. Li, Y. Gao, W. Yao, Z. Shuai, Z. An, X. Liu, W. Huang, Dynamic ultralong organic phosphorescence by photoactivation. *Angew. Chem. Int. Ed.* **57**, 8425–8431 (2018).
18. J. Yang, X. Zhen, B. Wang, X. Gao, Z. Ren, J. Wang, Y. Xie, J. Li, Q. Peng, K. Pu, Z. Li, The influence of the molecular packing on the room temperature phosphorescence of purely organic luminogens. *Nat. Commun.* **9**, 840 (2018).
19. K. Jiang, Y. Wang, C. Cai, H. Lin, Conversion of carbon dots from fluorescence to ultralong room-temperature phosphorescence by heating for security applications. *Adv. Mater.* **30**, 1800783 (2018).
20. S. Hirata, K. Totani, H. Kaji, M. Vacha, T. Watanabe, C. Adachi, Reversible thermal recording media using time-dependent persistent room temperature phosphorescence. *Adv. Opt. Mater.* **1**, 438–442 (2013).
21. Y. Su, S. Z. F. Phua, Y. Li, X. Zhou, D. Jana, G. Liu, W. Q. Lim, W. K. Ong, C. Yang, Y. Zhao, Ultralong room temperature phosphorescence from amorphous organic materials toward confidential information encryption and decryption. *Sci. Adv.* **4**, eaas9732 (2018).
22. S. Wan, W. Lu, Reversible photoactivated phosphorescence of gold(I) arylethynyl complexes in aerated DMSO solutions and gels. *Angew. Chem. Int. Ed.* **56**, 1784–1788 (2017).
23. C. Schweitzer, R. Schmidt, Physical mechanisms of generation and deactivation of singlet oxygen. *Chem. Rev.* **103**, 1685–1758 (2003).
24. T. Ogoshi, H. Tsuchida, T. Kakuta, T.-a. Yamagishi, A. Taema, T. Ono, M. Sugimoto, M. Mizuno, Ultralong room-temperature phosphorescence from amorphous polymer poly(styrene sulfonic acid) in air in the dry solid state. *Adv. Funct. Mater.* **28**, 1707369 (2018).
25. S. Reineke, F. Lindner, G. Schwartz, N. Seidler, K. Walzer, B. Lüssem, K. Leo, White organic light-emitting diodes with fluorescent tube efficiency. *Nature* **459**, 234–238 (2009).
26. F. Fries, M. Fröbel, S. Lenk, S. Reineke, Transparent and color-tunable organic light-emitting diodes with highly balanced emission to both sides. *Org. Electron.* **41**, 315–318 (2017).
27. V. I. Adamovich, S. R. Cordero, P. I. Djurovich, A. Tamayo, M. E. Thompson, B. W. D'Andrade, S. R. Forrest, New charge-carrier blocking materials for high efficiency OLEDs. *Org. Electron.* **4**, 77–87 (2003).
28. S. Reineke, N. Seidler, S. R. Yost, F. Prins, W. A. Tisdale, M. A. Baldo, Highly efficient, dual state emission from an organic semiconductor. *Appl. Phys. Lett.* **103**, 093302 (2013).
29. S. Reineke, M. A. Baldo, Room temperature triplet state spectroscopy of organic semiconductors. *Sci. Rep.* **4**, 3797 (2014).
30. H. D. Burrows, J. Seixas de Melo, C. Serpa, L. G. Arnaut, A. P. Monkman, I. Hamblett, S. Navaratnam, S_1~>T_1 intersystem crossing in π-conjugated organic polymers. *J. Chem. Phys.* **115**, 9601–9606 (2001).
31. V. Jankus, C. Winscom, A. P. Monkman, Dynamics of triplet migration in films of *N,N′*-diphenyl-*N,N′*-bis(1-naphthyl)-1, 1′-biphenyl-4, 4′′-diamine. *J. Phys. Condens. Matter* **22**, 185802 (2010).
32. B. Dickens, J. W. Martin, D. Waksman, Thermal and photolytic degradation of plates of poly(methyl methacrylate) containing monomer. *Polymer* **25**, 706–715 (1984).
33. R. H. G. Brinkhuis, A. J. Schouten, Thin-film behavior of poly(methyl methacrylates). 2. An FT-IR study of Langmuir-Blodgett films of isotactic PMMA. *Macromolecules* **24**, 1496–1504 (1991).
34. S. R. Tatro, G. R. Baker, K. Bisht, J. P. Harmon, A MALDI, TGA, TG/MS, and DEA study of the irradiation effects on PMMA. *Polymer* **44**, 167–176 (2003).
35. W. Marconi, A. Piozzi, R. Marcone, Synthesis and characterization of novel carboxylated ethylene-vinyl alcohol polymers. *Eur. Polym. J.* **37**, 1021–1025 (2001).
36. W. Qin, J. Liu, S. Chen, J. W. Y. Lam, M. Arseneault, Z. Yang, Q. Zhao, H. S. Kwok, B. Z. Tang, Crafting NPB with tetraphenylethene: A win–win strategy to create stable and efficient solid-state emitters with aggregation-induced emission feature, high hole-transporting property and efficient electroluminescence. *J. Mater. Chem. C* **2**, 3756–3761 (2014).
37. M. Muramatsu, M. Okura, K. Kuboyama, T. Ougizawa, T. Yamamoto, Y. Nishihara, Y. Saito, K. Ito, K. Hirata, Y. Kobayashi, Oxygen permeability and free volume hole size in ethylene–vinyl alcohol copolymer film: Temperature and humidity dependence. *Radiat. Phys. Chem.* **68**, 561–564 (2003).

Acknowledgments: We thank M. Kroll for the development of the automation of long-term measurements. **Funding:** This project has received funding from the European Research Council (ERC) under the European Union's Horizon 2020 Research and Innovation Program (grant agreement no. 679213 "BILUM"). **Author contributions:** H.T. and M.G. fabricated samples and performed measurements. M.G. wrote the manuscript. F.F. set up and took

photographs. S.R. supervised the project. H.T., M.G., F.F., and S.R. discussed results and contributed to the final editing. **Competing interests:** H.T., S.R., F.F., and M.G. are the inventors on a provision patent application with Technische Universität Dresden [no. 10 2018 214 374.9 (DE), filed 24 August 2018]. The authors declare no other competing interests. **Data and materials availability:** All data needed to evaluate the conclusions in the paper are present in the paper and/or the Supplementary Materials. Additional data related to this paper may be requested from the authors.

Submitted 10 July 2018
Accepted 13 December 2018
Published 1 February 2019
10.1126/sciadv.aau7310

Citation: M. Gmelch, H. Thomas, F. Fries, S. Reineke, Programmable transparent organic luminescent tags. *Sci. Adv.* **5**, eaau7310 (2019).

Programmable transparent organic luminescent tags

Max Gmelch, Heidi Thomas, Felix Fries and Sebastian Reineke

Sci Adv **5** (2), eaau7310.
DOI: 10.1126/sciadv.aau7310